

# **Widespread seismicity excitation throughout central Japan following the 2011 M=9.0 Tohoku earthquake, and its interpretation in terms of Coulomb stress transfer**

Shinji Toda<sup>1</sup>, Ross S. Stein<sup>2</sup>, Jian Lin<sup>3</sup>

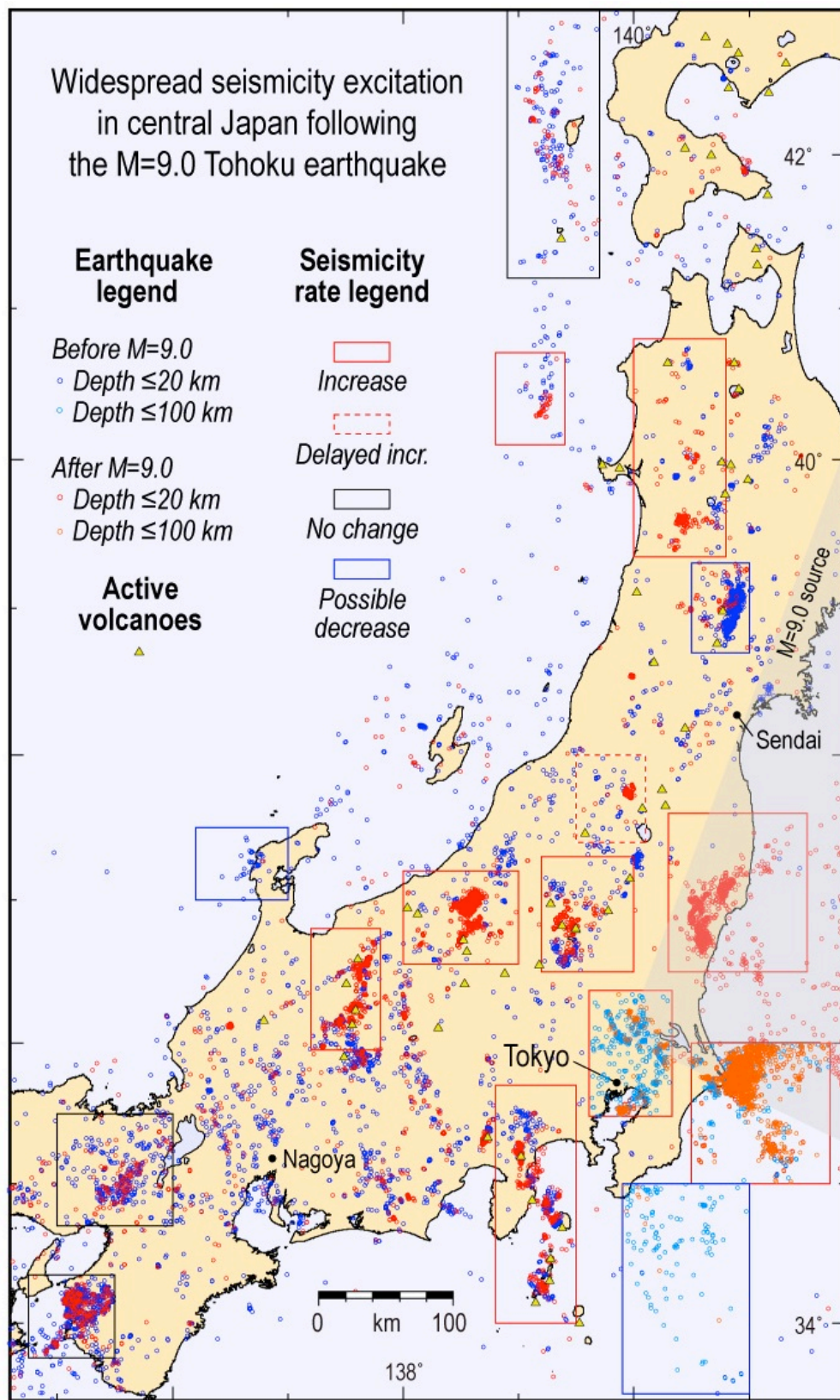
<sup>1</sup>Disaster Prevention Research Institute, Kyoto University, Japan

<sup>2</sup>U.S. Geological Survey, Menlo Park, California, USA

<sup>3</sup>Woods Hole Oceanographic Institution, Woods Hole, Massachusetts, USA

## ***Plain English Summary***

We report on a broad and unprecedented increase in seismicity rate for microearthquakes (magnitude  $\geq 2$ ) over a broad 600 by 200 km (360 by 120 mi) area across inland Japan, parts of the Japan Sea and the Izu islands, following the M=9.0 Tohoku mainshock. The seismicity increase occurs at distances of up to 425 km (360 mi) from the region of high ( $\geq 15$  m or 50 ft) seismic slip of the M=9 earthquake. While the origin and implications of the seismicity increase is subject to debate, its occurrence is beyond dispute. It was not seen for the 2004 M=9.1 Sumatra and 2010 M=8.8 Chile earthquakes, but they lacked the seismic networks necessary to detect such small events. Are these aftershocks, and if so what do they signify for the likelihood of large earthquakes across this region? Here we explore the possibility that the rate changes are the product of the stress transferred by the mainshock to small surrounding faults. Of the fourteen regions we can examine, seven show a positive association between calculated stress change and the observed seismicity rate change, three show a negative association (in opposition to our hypothesis), and the changes too small to assess in four regions. Regardless of the process that promotes the aftershocks, we argue that the microseismicity increases demonstrate that the ‘remote’ inland Japan and Japan Sea shocks (e.g., the Nagano Mw=6.3 earthquake on 3/12 03:59, the offshore-Noshiro Mw=6.2 on 3/12 04:46, the Mt. Fuji Mw=5.8 on 3/15, 22:31) are not exceptional. Rather than being isolated events, they are simply represent the largest shocks in a very broad zone of elevated seismicity rate.



From Toda, Stein & Lin, submitted to *Earth Planets Space*, 11 April 2011

# **Widespread seismicity excitation throughout central Japan following the 2011 M=9.0 Tohoku earthquake, and its interpretation in terms of Coulomb stress transfer**

Shinji Toda<sup>1</sup>, Ross S. Stein<sup>2</sup>, Jian Lin<sup>3</sup>

<sup>1</sup>Disaster Prevention Research Institute, Kyoto University, Japan

<sup>2</sup>U.S. Geological Survey, Menlo Park, California, USA

<sup>3</sup>Woods Hole Oceanographic Institution, Woods Hole, Massachusetts, USA

## **Abstract**

We report on a broad and unprecedented increase in seismicity rate for  $M \geq 2$  earthquakes following the M=9.0 Tohoku mainshock over inland Japan, parts of the Japan Sea and Izu islands, at distances of up to 425 km from the locus of high ( $\geq 15$  m) seismic slip on the megathrust. While the origin of the seismicity increase is subject to debate, its occurrence is beyond dispute. It was not seen for the 2004 M=9.1 Sumatra and 2010 M=8.8 Chile earthquakes, but they lacked the seismic networks necessary to detect such small events. Here we explore the possibility that the rate changes are the product of static Coulomb stress transfer to small faults. We use the nodal planes of  $M \geq 3.5$  earthquakes as proxies for such small active faults, and find that of fourteen regions averaging  $\sim 80$  by 80 km in size, half show a positive association between calculated stress changes and the observed seismicity rate change, three show a negative correlation, and four show changes too small to assess. This work demonstrates that seismicity can turn on in the nominal stress shadow of a mainshock as long as small geometrically diverse active faults exist there, which is likely quite common.

## 1. Introduction

The  $M=9.0$  Tohoku-chiho Taiheiyo (hereafter, 'Tohoku') earthquake caused measurable crustal deformation throughout northeastern and central Japan (Geospatial Information Authority of Japan, 2011) as a result of slip on the 500-km-long and 200-km-wide seismic megathrust source (e.g., Wei *et al.*, 2011). Many offshore aftershocks, including four  $M \geq 7$  and  $\sim 70$   $M \geq 6$  shocks, have struck during the ensuing three weeks. The possibility of other large subsequent earthquakes on adjacent portions of the megathrust, similar to the 28 March 2005  $M_w=8.6$  Simeulue-Nias earthquake following the 26 December 2004  $M_w=9.1$  Sumatra-Andaman earthquake (Nalbant *et al.*, 2005; Pollitz *et al.*, 2006) is thus quite threatening. Sites of subsequent large earthquakes with a tsunami potential include the Sanriku-Hokubu area to the north, and Off-Boso (east of the Boso peninsula) to the south (Headquarters for Earthquake Research Promotion, 2005) of the 2010 Tohoku rupture.

Equally important for the exposed population and infrastructure would be the occurrence of large inland shocks in northern Honshu. Among such inland sites, none is more important than Tokyo, which was last struck by the Kanto  $M=7.9$  Sagami megathrust event in 1923 (Nyst *et al.*, 2006), and a deeper inland event in the 1855  $M \sim 7.2$  Ansei-Edo earthquake (Grunewald and Stein, 2006). The concern for triggered inland earthquakes is heightened by several inland large earthquakes in Tohoku that have followed  $M=7-8$  interplate events by months to a decade (Shimazaki, 1978; Seno, 1979; Churei, 2002).

Among these is the 31 August 1896  $M_j=7.2$  Rikuu earthquake, which produced a 30-km-long surface rupture that devastated the eastern Akita Prefecture (with 200 deaths). Three  $M\sim 6$  shallow inland earthquakes have already struck as far as  $\sim 300$  km from the  $M=9$  source within five days of the Tohoku mainshock, reaffirming the broad reach and triggering potential of the great quake.

To evaluate the potential triggering impact of the Tohoku earthquake to inland Japan, we analyze the seismicity rate change since the Tohoku mainshock, and calculate the static Coulomb stress changes caused by the Tohoku mainshock over the region of seismicity rate change.

## **2. Inland Seismicity Rate Changes Associated with the Tohoku Earthquake**

We use the preliminary hypocenter list (PDE) provided by JMA to examine the seismic response to the Tohoku earthquake. The PDE catalog normally lists the earthquakes that have occurred until two days before present. However, because of the enormous number of aftershocks since March 11, human inspection of the records is incomplete, as can be seen by an inflection point in the curves for the a cumulative number of shocks about a week after the mainshock (time series in Fig. 1). Even during the first week after March 11, data transfer interruptions caused by seismic station power outages and damage in northern Tohoku may affect the earthquake record, and thus apparent

seismicity rate drops might be artifacts. In contrast, the sudden seismicity rate jumps are likely real, even if as yet we cannot determine their total duration. Some of the rate increases, such as boxes J and M (Fig. 1), exhibit gradual declines since March 11 reminiscent of aftershock sequences.

Broadly, there are strong increases in seismicity rate across a region extending up to 300 km from the distal edges of the  $M=9$  rupture surface, and 425 km from the locus of high ( $\geq 15$  m) seismic slip. This widespread seismic excitation is unprecedented, although it should be noted that for the roughly-equivalent  $M=9.1$  Sumatra, Indonesia, and  $M=8.8$  Maule, Chile, earthquakes, no  $M < 4.7$  earthquake could be detected (the Global CMT and NEIC detection threshold), and so these preliminary Tohoku observations offer an unmatched record of earthquake triggering. Further, remote earthquake triggering was observed at even great distances, but much lower densities, following the 1992  $M=7.3$  Landers and 2002  $M=7.9$  Denali, earthquakes (Hill, 2008). In addition to the microseismicity, an  $M_j=6.7$  earthquake occurred 13 hours after the Tohoku mainshock in box J (Fig. 1), a  $M_j=6.4$  earthquake occurred 24 hours after the Tohoku earthquake in box A, and a  $M_j=6.4$  earthquake struck about 4.5 days after the Tohoku earthquake at the base of Mt. Fuji. At first glance it would appear that these remote earthquakes are distinct from aftershocks closer to the rupture plane, but examination of Fig. 1 reveals that it is more likely that they are simply the largest events to occur within the broad zone of increased seismicity rate.

Sudden increases of seismicity observed in regions B (Akita), E (southern Fukushima – northern Ibaraki), F (Cape Inubou), H (Mt. Hotaka-Mt. Asahi), I (Kanto), where a burst of seismicity began in the head of Tokyo Bay several days after the Tohoku shock, M (Izu and islands), and K (Hida mountain range) (Fig. 1). A possible increase in seismicity rate delayed by 1-3 days is observed in the box D. The increase in seismicity in regions J and A could be masked by aftershocks of the  $M \sim 6$  mainshocks, or the larger events could be part of the same process.

### **3. Calculation of the Coulomb Stress Change**

The static Coulomb stress change caused by a mainshock has been widely applied to assess areas of subsequent off-fault aftershocks since the 1990s (e.g., Reasenber and Simpson, 1992). The Coulomb stress change is defined as  $\Delta CFF = \Delta \tau + \mu \Delta \sigma$ , where  $\tau$  is the shear stress on the fault (positive in the inferred direction of slip),  $\sigma$  is the normal stress (positive for fault unclamping), and  $\mu$  is the apparent friction coefficient. Failure is promoted if  $\Delta CFF$  is positive and inhibited if negative; both increased shear and unclamping of faults are taken to promote failure, with the role of unclamping modulated by fault friction.

To resolve the Coulomb stress change on a ‘receiver fault’ (fault receiving stress from a mainshock) requires a source model of the earthquake fault slip, as well as the geometry and slip direction on the receiver. A simple approach is to assume that the receiver faults share the same strike, dip and rake as the mainshock source fault, or one can resolve stress on a major fault of known geometry (e.g., McCloskey *et al.*, 2003). Another approach is to find the receiver faults at every point that maximize the Coulomb stress increase given the earthquake stress change and the tectonic stress (King *et al.*, 1994), termed the ‘optimally-oriented’ Coulomb stress change. However, the M=9.0 Tohoku earthquake at least temporarily raised the seismicity rate across a region so large that various tectonic stress fields associated with the complex convergence of three tectonic plates are intermingled. One approach in such a case is to resolve the stress change on major active faults (Toda *et al.*, 2011, this issue) based on their inferred geometry and slip sense. While this is instructive as a guide to the likelihood that one of these major faults could rupture, the faulting mechanisms of small to moderate shocks that dominate the local seismicity are undoubtedly more complex and varied than the associated major structures, and so we do not use it here. Instead, we propose an alternative.

#### **4. Use of Focal Mechanisms as Proxies for Small Active Faults**

Here we propose to resolve the Coulomb stress changes on the nodal planes of the abundant small earthquakes as proxies for active faults. We make use of fault plane

solutions of the 14-year-long F-net catalog (NIED, 2011), which for inland Japan principally includes shallow crustal earthquakes of  $M_j \geq 3.5$ ; this corresponds to source dimension  $\geq 400$  m (Wells and Coppersmith, 1994). The value of this approach is evident in Fig. 2a and Fig. 3a by comparing the mapped active faults (green lines) with the focal mechanisms: Even though the mapped faults (Research Group for Active Faults in Japan, 1991) often have sinuous and en echelon traces, the focal mechanisms reveal even more complexity, such as strike-slip faults amid the mapped thrust faults of Tohoku, or thrust mechanisms with a wide range of strikes at the site of the 2008  $M_j=7.2$  Iwate-Miyagi Nairiku earthquake (box C in Fig. 2a).

In Toda *et al.* (2011, this issue), we tested six representative source models and three friction values to determine which model produces the greatest gain in aftershock mechanisms promoted by the mainshock relative to the background (pre-Tohoku) mechanisms. The Wei *et al.* (2011) source model and a friction of 0.4 produces the greatest (62%) gain, and so we use them here to calculate the stress changes in an elastic half space (Okada, 1992) with Poisson's ratio 0.25 and shear's modulus  $3.2 \times 10^5$  bar. We resolve the static Coulomb stress change on both nodal planes at each hypocenter; calculations on both planes are needed because the normal stress change is different on each plane in a set, and we do not know which of the two nodal planes slipped. Both are used in the statistical summaries in Table 1. In Figs. 2b and 3b, we plot the maximum Coulomb stress change for the most positive plane only (we would otherwise have to plot

both sets of planes), and also place positive changes (red dots) atop negative changes (blue dots) where earthquakes overlap. Thus, the figures have an intentional ‘red bias,’ but Table 1 uses both nodal planes and has no bias. We examine 14 rectangular areas where the seismicity is abundant (Fig. 1) and where focal mechanisms are available (Figs. 2a and 3a).

## **5. Comparison of Seismicity Rate Changes and Coulomb Stress Changes**

Comparison of Fig. 1 with Figs. 2b and 3b indicates positive associations between observed seismicity rate increases and Coulomb stress increases resolved on nodal planes in seven of the 14 boxes. We find no clear changes in either seismicity rate or stress in 4 boxes, and negative correlations in 3 boxes (Table 1).

The positive correlations include boxes F and I straddling the rupture, box M located 150-225 km from the rupture surface, and box K, 250 km from the rupture edge. In box I (Kanto district), we included mechanisms as deep as 100 km because of the complex plate configuration beneath Tokyo (Toda *et al.*, 2008). More than 80% of the stress changes for mid to deeper shocks along the NS-trending ‘Kanto seismic corridor’ (box I) are positive.

There is also a correlation between the (albeit preliminary) seismicity rate decreases and stress decreases in boxes C, G and L. Detecting seismicity rate decreases normally

demands not only a high rate of preceding seismicity, but also a long post-mainshock catalog that is not yet available. Box C was the site of the 2008  $M_j=7.2$  Iwate-Miyagi Nairiku earthquake, and box L was the site of the 2007  $M_j=6.8$  Noto Hanto earthquake; to be certain that these sites sustained seismicity rate drops, one would need to remove the expected decaying aftershock frequency from the time series, which we have not yet done. Nevertheless, the aftershock frequency decay 3-4 years after the mainshocks is low, and the observation period in Fig. 1 is brief, and so the time series in Fig. 1 for at least box L appears convincing as long as post-Tohoku earthquakes are not missing from the catalog.

Inconsistent with the static stress hypothesis, box D shows a delayed rate increase but no stress increase, and there are seismicity rate increases in box A for which Coulomb stress increases are present but do not dominate. Box B lacks sufficient focal mechanisms for confident assessment. Box J, chosen to be centered on the  $M_j=6.7$  shock 13 hr after the mainshock, shows a rate increase but a stress decrease. (Boxes N, O and P show little or no seismicity rate change or stress change; they lie up to 600 km from the Tohoku rupture.) Box E is not analyzed because the post-Tohoku seismicity is associated with shallow normal faulting, whereas the focal data contain only deep reverse mechanisms.

A majority of the mechanisms along the Ou backbone mountain range (boxes B, C and D in Fig. 2b) are thought to be north-striking thrust faults, which would lie in the principal

stress shadow of the Tohoku mainshock, and thus be brought farther from failure (Toda *et al.*, this issue). However, the significant percentage of strike-slip mechanisms and thrusts of divergent strikes result in a large number of positive stress changes. This underscores that resolving stress on the major faults alone oversimplifies and idealizes the much more complex stress transfer.

## **6. Discussion and Conclusions**

The fundamental observation driving this study is the widespread seismicity rate increase across inland Japan, and extending to some portions of the Japan Sea and to the Izu island chain. Remarkably, seismicity turned on at distances of up to 300 km from the lower edge of the Tohoku earthquake rupture surface, and up to 450 km from the high (<15 m) slip zone. These seismicity rate increases are apparent for  $M \geq 2$  earthquakes, about half the boxes include  $M \geq 4$  earthquakes and in four cases are punctuated by  $M=5-6$  earthquakes. Most of these seismicity increases follow the Tohoku mainshock immediately, but some were delayed by up to several days. These distant aftershocks could be triggered dynamically, or they could be caused by the static stress changes. But the maximum triggering distance, less than two source dimensions from the mainshock, is consistent with the global absence  $M \geq 5$  shocks triggered at distances greater distances (Parsons and Ammon, 2011). Here we explored the static hypothesis, which we adapted to the special circumstances of triggering on very small faults that are neither optimally oriented in the regional stress field nor parallel to the major faults. We thus use the

Coulomb stress change resolved on the nodal planes of the smallest earthquakes with focal mechanisms, which limits us to  $M \geq 3.5$  shocks, a  $\geq 400$  m rupture scale that at least overlaps that of the aftershocks.

A tentative examination of the observed seismicity rate changes and calculated Coulomb stress changes has met with promising but certainly incomplete success, since we find seven positive correlations and three negative correlations (Table 1). Three of the correlations derive from decreases both in observed seismicity rate and calculated Coulomb stress, and while we are confident in the calculated stress decreases, it is perhaps too soon to be confident in the seismicity rate declines.

Regardless of the process that promotes the aftershocks, we argue that the microseismicity increases demonstrate that the ‘remote’ Japan Sea and inland Japan shocks (e.g.,  $M_w=6.3$  on 3/12 03:59,  $M_w=6.2$  on 3/12 04:46,  $M_w=5.8$  on 3/15, 22:31) are not exceptional; in fact they are not truly isolated events. Instead, they simply represent the largest shocks in a very broad zone of elevated seismicity rate that is evident for  $M \geq 2$  earthquakes.

One of the greatest surprises of this work is that the effect of the stress shadow expected in Tohoku for north-striking thrust fault appears—as yet—largely absent. Instead, much but not all of Tohoku exhibits an increased rate of seismicity. Here we find that this

behavior is nevertheless consistent with static Coulomb stress transfer, but to smaller faults with geometries different from the major faults, an argument first advanced by Marsan (2006). One important question is whether the activation of these smaller divergent faults could trigger a large event on one of the major thrusts. This appears to have occurred when the 15 June 1986  $M \sim 8\frac{1}{4}$  offshore Sanriku earthquake was succeeded by the 31 August 1896  $M_j=7.2$  Rikuu inland earthquake at the same latitude (box B, Fig. 2a). Since the 2011 Tohoku mainshock is about ten times larger than the Meiji Sanriku mainshock, there could be unprecedented changes in intraplate seismicity during the months to years ahead.

**Acknowledgements.** We thank David Hill and Andrea Llenos for thoughtful reviews, and we are grateful to JMA and NIED for the preliminary hypocenter list and focal mechanisms.

## References

- Churei, M., Relationships between eruptions of volcanoes, inland earthquakes ( $M \geq 6.2$ ) and great tectonic earthquakes in and around north-eastern Japan Island arc, *J. Geography*, **111**, 175-184, 2002.
- Geospatial Information Authority of Japan, The 2011 off the Pacific coast of Tohoku earthquake: Crustal deformation and fault model (preliminary), <http://www.gsi.go.jp/cais/topic110313-index-e.html>, 2011.
- Grunewald, E., and R. S. Stein, A new 1649-1884 catalog of destructive earthquakes near Tokyo and implications for the long-term seismic process, *J. Geophys. Res.*, **111**, doi:10.1029/2005JB004059, 2006.
- Headquarters for Earthquake Research Promotion, Report: 'National Seismic Hazard Maps for Japan (2005)', 162 pp, <http://www.jishin.go.jp/main/index-e.html>, 2005.
- Hill, D. P., Dynamic stresses, Coulomb failure, and remote triggering, *Bull. Seismol. Soc. Amer.*, **98**, 66-92, doi:10.1785/0120070049, 2008.
- King, G. C. P., R. S. Stein, and J. Lin, Static stress changes and the triggering of earthquakes, *Bull. Seismol. Soc. Am.*, **84**, 935-953, 1994.
- Marsan, D. Can coseismic stress variability suppress seismicity shadows? Insights from a rate-and-state friction model *J. Geophys. Res.* **111**, B06305, doi:10.1029/2005JB004060, 2006.
- McCloskey, J. Nalbant, S. S., S. Steacy, C. Nostro, O. Scotti, and D. Baumont, Structural constraints on the spatial distribution of aftershocks, *Geophys. Res. Lett.*, **30**, doi:10.1029/2003GL017225, 2003.
- Nalbant, S. S., S. Steacy, K. Sieh, D. Natawidjaja, and J. McCloskey, Earthquake risk on the Sunda trench, *Nature*, **435**, 756-757, 2005.
- National Research Institute for Earth Science and Disaster Prevention (NIED), Broadband Seismograph Network (F-net), <http://www.fnet.bosai.go.jp/top.php?LANG=en>
- Nyst, M., T. Nishimura, F. F. Pollitz, and W. Thatcher, The 1923 Kanto earthquake re-evaluated using a newly augmented geodetic data set, *J. Geophys. Res.*, **111**, B11306, doi:10.1029/2005JB003628, 2006.

- Parsons, T., and A.A. Velasco, Absence of remotely triggered large earthquakes beyond the mainshock region, *Nature Geoscience*, **4**, doi:10.1038/ngeo1110, 2011.
- Okada, Y., Internal deformation due to shear and tensile faults in a half-space, *Bull. Seismol. Soc. Am.*, **82**, 1018-1040, 1992.
- Pollitz, F. F., P. Banerjee, R. Burgmann, M. Hashimoto, and N. Choosakul, Stress changes along the Sunda trench following the 26 December 2004 Sumatra-Andaman and 28 March 2005 Nias earthquakes, *Geophys. Res. Lett.*, **33**, L06309, doi:10.1029/2005GL024558, 2006.
- Reasenbergs, P. A., and R. W. Simpson, Response of regional seismicity to the static stress change produced by the Loma Prieta earthquake, *Science*, **255**, 1687-1690, 1992.
- Research Group for Active Faults in Japan, Active Faults in Japan, sheet maps and inventories, rev. ed., 437 pp., Univ. Tokyo Press, Tokyo, 1991.
- Seno, T., Intraplate seismicity in Tohoku and Hokkaido and large interplate earthquakes: A possibility of a large interplate earthquake off the southern Sanriku coast, northern Japan, *J. Phys. Earth*, **27**, 21-51, 1979.
- Shimazaki, K., Correlation between intraplate seismicity and interplate earthquakes in Tohoku, northeast Japan, *Bull. Seismol. Soc. Am.*, **68**, 181-192, 1978.
- Toda, S., R. S. Stein, S. H. Kirby, and S. B. Bozkurt, A slab fragment wedged under Tokyo and its tectonic and seismic implications, *Nature Geoscience*, **1**, 771-776, doi:10.1038/ngeo318, 2008.
- Toda, S., J. Lin, R. S. Stein, Using the 2011 M=9.0 Tohoku earthquake to test the Coulomb stress triggering hypothesis and to calculate faults brought closer to failure, submitted to this issue in *EPS*, 2011.
- Wells, D. L., and K. J. Coppersmith, New empirical relationships among magnitude, rupture length, rupture width, rupture area, and surface displacement, *Bull. Seismol. Soc. Amer.*, **84**, 974-1002, 1994.
- Wei, S. and A. Sladen, and the ARIA group, Updated result, 3/11/2011 (Mw 9.0), Tohoku-oki, Japan, [http://tectonics.caltech.edu/slip\\_history/2011\\_taiheiyo-oki/index.html](http://tectonics.caltech.edu/slip_history/2011_taiheiyo-oki/index.html), 2011.

**Table 1**

Box Fig. 1	Min. Lon. (°)	Max. Lon. (°)	Min. Lat. (°)	Max. Lat. (°)	% positive $\Delta$ CFF *	Ave. DCFF (bar)	Seismicity Rate Change	Correlation between rate change and $\Delta$ CFF
A	138.80	139.40	40.10	40.70	27	-0.22	Increase	Negative
C	140.50	141.00	38.70	39.30	11	-3.3	Decrease	Positive
D	139.50	140.10	37.40	38.00	14	-1.3	Delayed increase	Negative
F	140.50	141.70	35.00	36.00	75	2.5	Increase	Positive
G	139.90	141.00	33.50	35.00	37	-0.04	Decrease	Positive
H	139.20	140.00	36.50	37.30	47	0.1	Increase	—
I	139.61	140.33	35.48	36.37	83	1.2	Increase	Positive
J	138.00	139.00	36.50	37.20	15	-0.4	Increase	Negative
K	137.20	137.80	35.95	36.80	88	0.3	Increase	Positive
L	136.20	137.00	37.00	37.50	19	-0.11	Decrease	Positive
M	138.80	139.50	34.00	35.70	82	0.1	Increase	Positive
N	138.90	139.70	41.20	43.00	59	0.05	No change	—
O	135.00	136.00	34.70	35.50	17	-0.04	No change	—
P	134.75	135.50	33.75	34.35	47	0	No change	—

\*  $\Delta$ CFF positive > 50% (red); <50% (blue). Ave.  $\Delta$ CFF value > 0 (red); <0 (blue)

The percentage of nodal planes (two for each earthquake) with Coulomb stress increases and the associated average stress change is compared with the observed seismicity rate change. Because of the preliminary state of the aftershock catalog, we have not yet calculated correlation coefficients, and so the correlations are approximate.

**Figure captions**

**Figure 1.** Seismic response of inland Japan to the M=9.0 Tohoku mainshock. Cumulative numbers of  $M_j \geq 0.0$  earthquakes during 1/1–3/31/2011 are plotted as the blue curve for selected boxed areas in the map, using the preliminary hypocenters of the JMA catalog (downloaded on 4/8/2011). The corresponding time series of earthquakes are represented by green stems proportional to magnitude. The catalog is likely complete for  $M \geq 2.0$ .

**Figure 2.** Coulomb stress changes resolved on the nodal planes of small earthquakes as proxies for small active faults in Tohoku, Kanto and Shin'etsu districts. (a) Focal mechanisms from the F-net catalog (NIED, 2011) since 1997 (depth  $\leq 20$  km for inland areas,  $\leq 50$  km for the eastern margin of Japan Sea region, and  $\leq 100$  km for Kanto); D is depth. (b) Maximum Coulomb stress change chosen from each pair of nodal planes; where earthquakes overlap, the most positively-stressed shocks are plotted atop. The color of the box boundaries follows the convention of Fig. 1.

**Figure 3.** Coulomb stress changes resolved on the nodal planes of the background earthquakes as proxies of local or regional fault structure in Chubu and Kinki districts. (a) Fault plane solutions in the F-net catalog (NIED, 2011) since 1997 (depth  $\leq 20$  km). (b) Maximum Coulomb stress change chosen from each pair of nodal planes.

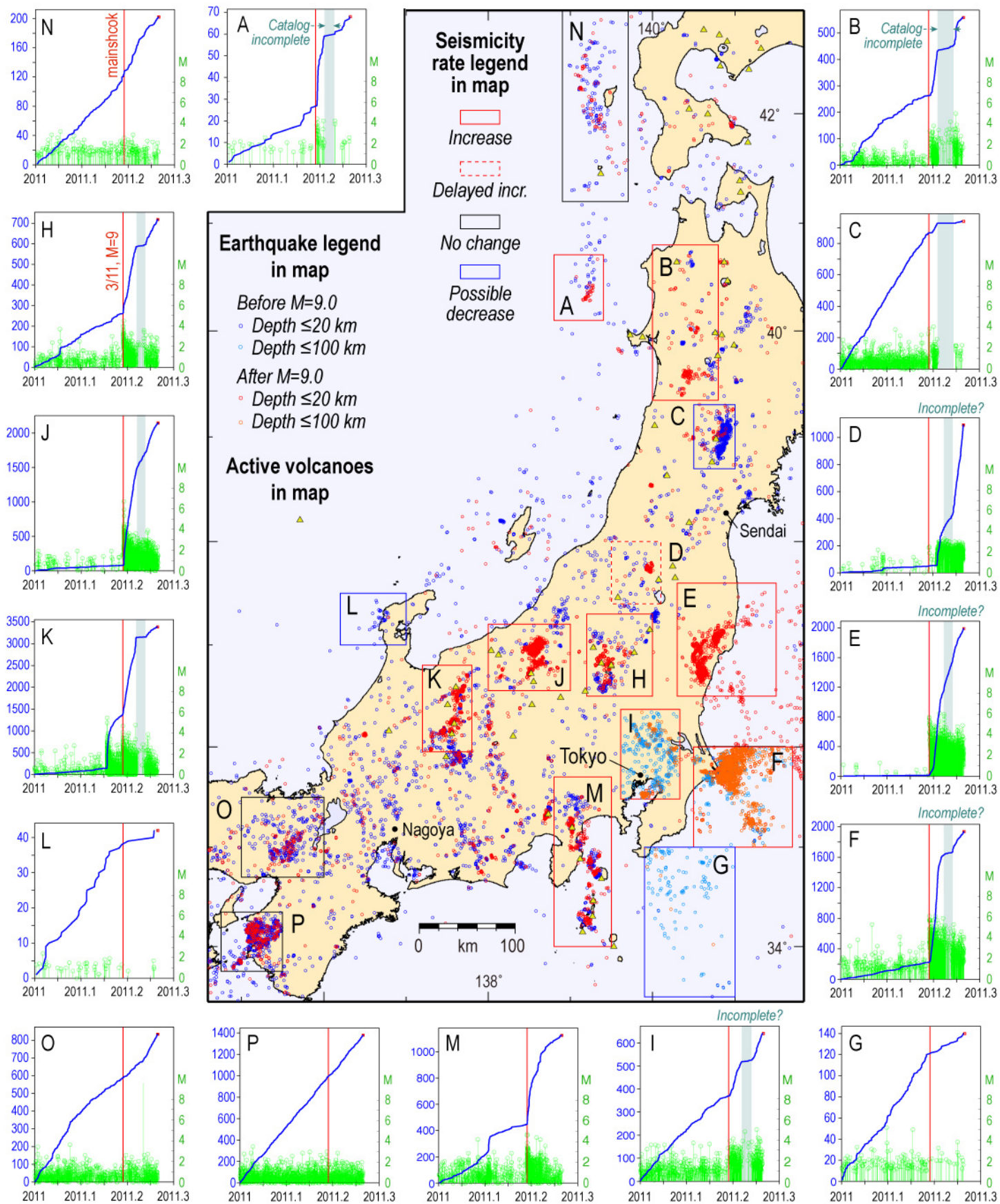


**Fig. 1**

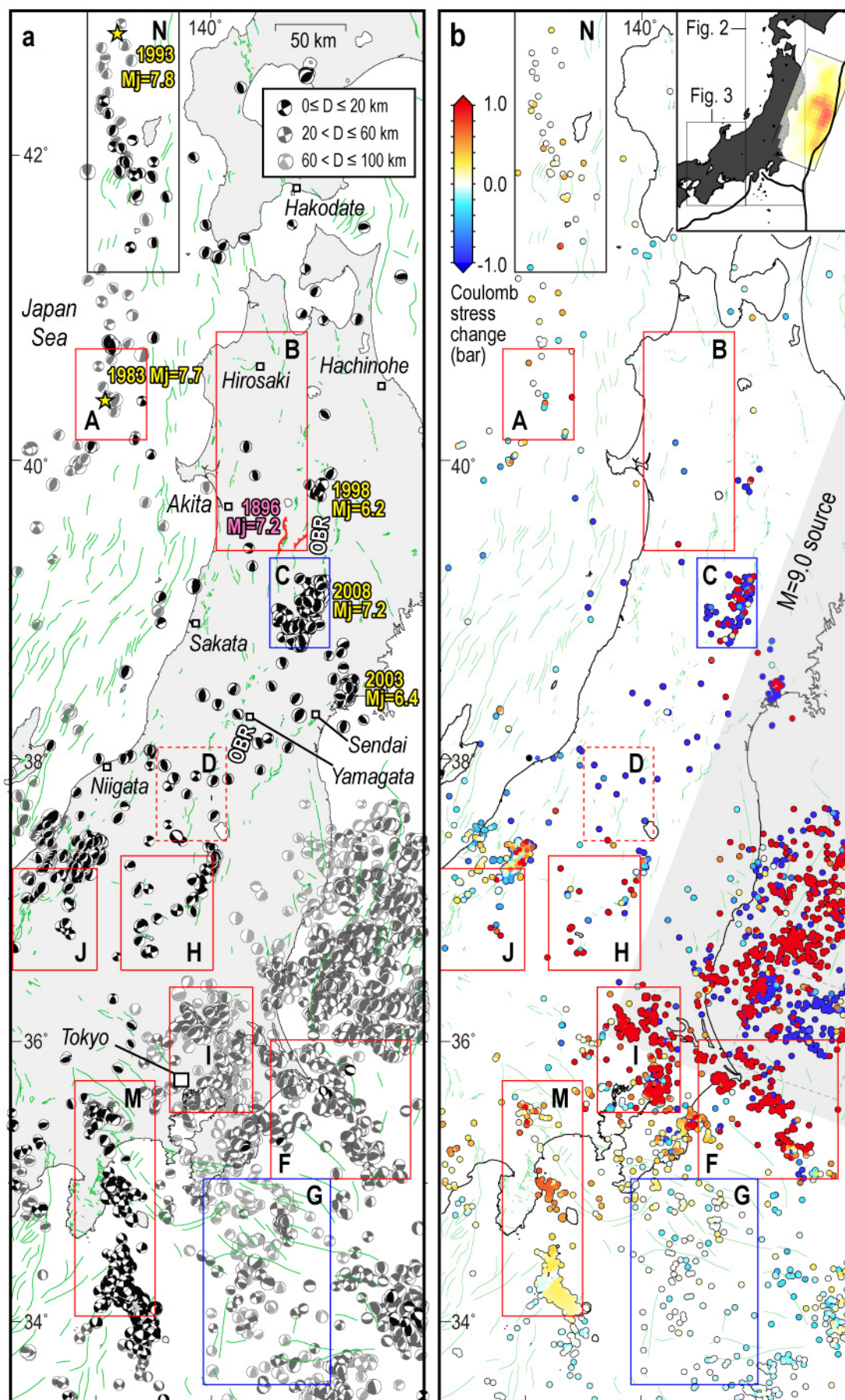


Fig. 2

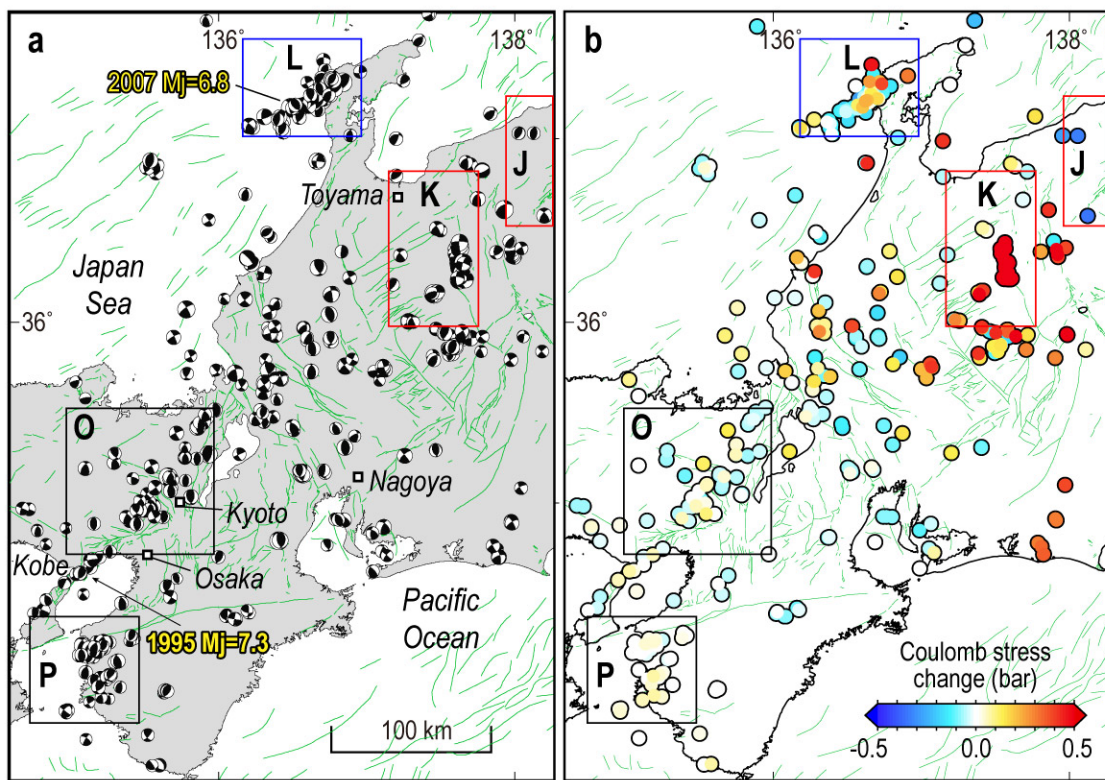


Fig. 3